

## LARGE APERTURE SUPERCONDUCTING CRYOSTABLE QUADRUPOLES FOR CEBAF'S HIGH MOMENTUM SPECTROMETER

S.R. Lassiter, P.D. Brindza, W.T. Hunter, R.R. Thorpe,  
M.J. Fowler, J.A. Miller  
Continuous Electron Beam Accelerator Facility  
12000 Jefferson Avenue  
Newport News, VA 23606

### Abstract

The present design for CEBAF'S Hall C High Momentum Spectrometer<sup>1,2</sup> calls for two large aperture quadrupoles, each having the same physical characteristics but operating at different field gradients. A cold-iron, superconducting, laminated yoke magnet has been developed as the reference design. The results of the two and three dimensional magnetostatic studies will be presented here along with some details of the conductor and cryostat design.

### Introduction

It is our intention here at CEBAF to purchase from industry, the magnets for the HMS spectrometer based upon magnetic performance specifications. This paper will present a reference design that we believe will meet the specifications listed in Table 1 below.

The design of Q2/Q3 was also constrained by other non-optical requirements such as size and weight of the magnet, cryostability, low current, and low power lead consumption. The magnetostatic analyses were performed for the requirements of the larger gradient Q2 magnet.

TABLE 1. Q2/Q3 Optical Requirements and Magnet Specifications

	Q2	Q3
Leff	= 210 cm	210 cm
Field Gradient	= 445.7 G/cm	194 G/cm
R(pole)	= 35 cm	35 cm
R(good field region)	= 30 cm	30 cm
Field @ Pole	= 1.56 Tesla	.68 Tesla
Dynamic Field range	= 10:1	
Integral Multipole Field errors (percent of quadrupole):		
Dodecapole(at pole)	< 3.0%	< 3.0%
Unknown Multipoles (within aperture)	< 0.3%	< 0.5%
Physical Length	= 3.0 m	
Iron Length	= 1.84 m	
Diameter of yoke	= 1.40 m	
Length/Bore ratio	= 5.5	
Weight of yoke	= 15 tons	

### Geometry

The cold iron design of Q2/Q3 is based upon the conformal mapping of a window frame dipole into a quadrupole geometry. This method was used in the reference design of the smaller front end quadrupole Q1 of the HMS.<sup>3</sup> Figure 1 shows a cross section view of the Q2/Q3 quadrupole magnet.

Manuscript received September 24, 1990

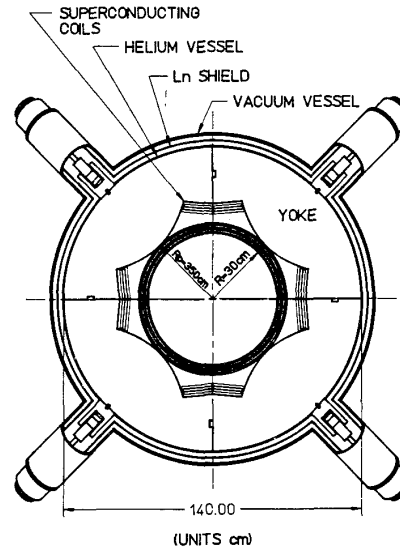


FIGURE 1. CROSS SECTIONAL VIEW OF Q2/Q3, SHOWING INNER AND OUTER CRYOSTAT. POLE RADIUS = 35cm

### Yoke Design

Attention was given to the overall size of the yoke and to the field levels within the yoke. The field levels were controlled by sizing the width of the smallest flux path within the yoke to be equal to one half of the flux path length along the pole face for a field level of 1.6 Tesla, as shown in Figure 2. The magnetic properties of the yoke were taken from the internal table of POISSON<sup>4</sup>. This is listed as 1006 iron at 4.2 kelvin.

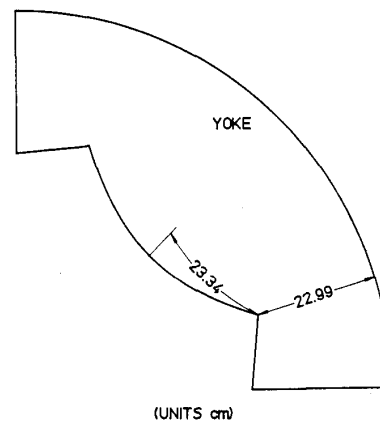
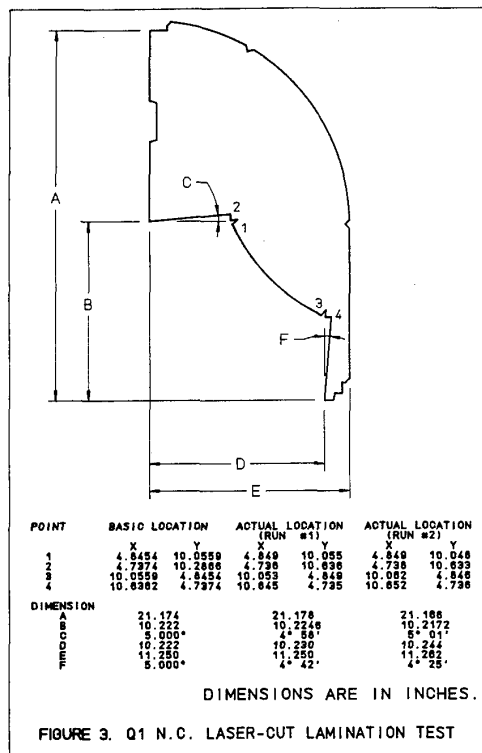


FIGURE 2. 1/4 GEOMETRY OF Q2/Q3 SHOWING THE FLUX PATH LENGTH IN THE YOKE AND ALONG THE POLE FACE.

We have investigated the process of numerically controlled laser cutting for the yoke/pole laminations as it relates to cost effectiveness and cutting precision. The tolerance control of the pole shape is of prime concern, as the field quality is determined as much by the pole shape as it is by the current distribution. Actual laser cut laminations were made for the Q1 geometry. Figure 3 gives the accuracy of this test fabrication. The machining tolerance of the laminations when modeled in POISSON were well within the magnetostatic specifications.



### Cryostat Design

The transition from warm to cold occurs over the spatial dimension of 5. cm inside the bore of the magnet. The inner warm bore will be a stainless steel cylinder wrapped in super-insulation to reduce the radiation heat load to the inflated stainless steel liquid nitrogen intercept panel. The helium stainless cylinder will also be wrapped with super insulation to reduce radiation heat loads. The cylinders will share a common vacuum between them to lower thermal conduction.

The magnet will be cooled by means of a natural thermal syphon supplied from a helium reservoir mounted above the magnet. The capacity of the reservoir is sized such that a 3 hour supply of liquid helium will be available in the event of short duration supply interruptions.

The cold iron yoke will be supported within the cryostat by eight constant tension support links that attach from the end of the laminations to standoffs attached to the outer vacuum vessel<sup>5</sup>. The link will be intercepted by a liquid nitrogen thermal shield to reduce heat conduction down the shaft.

### Super Conductor Design

The Q2/Q3 quadrupole conductor is a multi-filament, .023 cm diameter, NbTi-copper, 11-strand Rutherford cable. This cable is then extruded into a high purity aluminum stabilizer (99.999 Al.) for cryostability. Figure 4 shows a cross sectional view of the conductor.

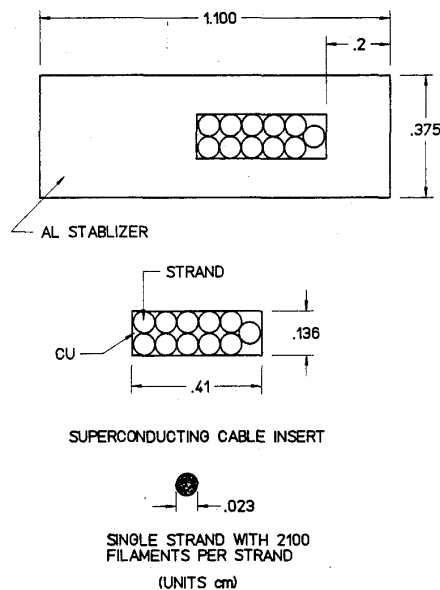


Table 2. Q2/Q3 cryostable conductor Parameters

Beam energy	= 6.0 Gev
NI/pole	= 217310 Amp Turns
# Turns/pole	= 71
Turn Length	= 465 cm
I/turn	= 3.061 KAmps
Ic/turn	= 4.62 KAmps
Al/Cu/NbTi	= 6.4/1.8/1
Stekly #	= .45
Stored Energy	= .31 MJ/m (Q2 at 1.56 Tesla)
Power Lead Consumption	= 9.1 L of helium/hour

For the Stekly calculation, no credit was taken for the copper present in the strands.

As increases in the beam energy for CEBAF look promising, the cryostability of the magnet is preserved up to the operating current of 4.6 KAmps, corresponding to a beam energy of 7.5 GeV/c.

### Two Dimensional Quadrupole Field Calculations

The initial magnetostatic solutions were performed using the code POISSON to gain an understanding of the sensitivity of the 2-dimensional problem to coil and iron geometries. The need to allow for adequate helium flow passage channels in and around the coil stacks was used as a constraining parameter in minimizing the unwanted multipoles.

Three stacks of conductor were used to achieve the desired amp turns and lower the operating current. Gaps along the median plane for each coil stack were constrained to be equal in an attempt to reduce the number of individual parameters that could effect field quality. The heights of each coil stack were individually sized to reduce field errors. This results in an unequal number of turns per coil stack as well as the need for an additional spacer in the first two stacks. The turn to turn insulation consists of 2.2 mm thick G-10 spacers sized such that adequate helium flow would result as well as maximizing the current density. The spacing between the stacks of conductor was sized such that the width of the coils stacks would be kept to a minimum yet provided for sufficient helium flow along the stack heights. The superconducting cable is offset within the aluminum stabilizer as an aid in reducing the unwanted harmonics. The spacing between the coil stack and the iron yoke was also used to achieve a better field quality.

The current carrying portions of the conductor were modeled as uniform stacks in all of the magnetostatic analysis. Figure 5 shows the approximation to the current carrying portions of the conductor that were modeled in the magnetostatic problems.

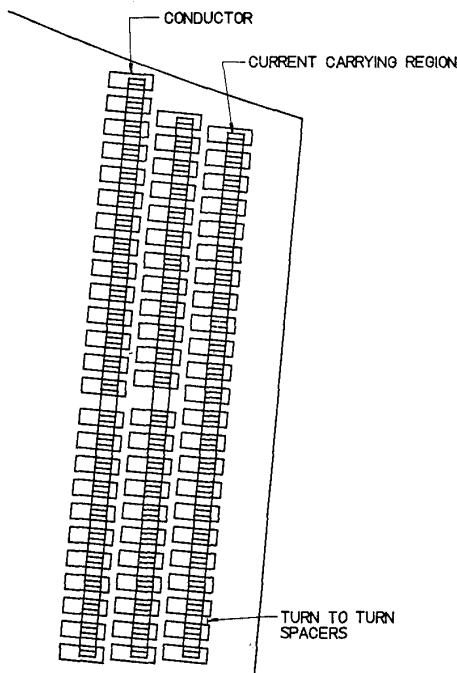


FIGURE 5. CURRENT CARRYING REGIONS AS MODELED IN POISSON AND TOSCA

Table 3 lists the coefficients of the field multipoles at a radius of 35. cm and a beam energy of 6.0 GeV/c.

Table 3. Poisson Harmonic Analysis

N	B(N)	B(N)/B(2) %
2	1.5540E+04	1.0000
6	6.8937E+00	0.0444
10	-1.0264E+01	-0.0776
14	-2.0747E+01	-0.1335

$2 \times N = \text{multipole}$

Field is given by  $B = \text{Sum} [B(N) \cdot (r/R_p)^{(N-1)}]$

The field within the iron yoke was 1.45 Tesla along the median axis and 1.6 Tesla at the pole. Flux leakage outside the iron was 6.5 Gauss next to the yoke and drops to 4.8 Gauss 30 cm away at the boundary. Figure 6 shows the 2-dimensional solution for one-eighth of the geometry from POISSON.

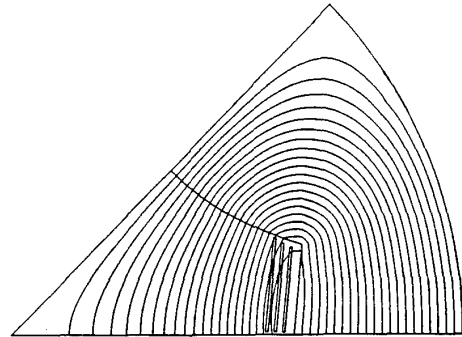


FIGURE 6. FIELD LINES AND GEOMETRY FROM POISSON

### 3-Dimensional Quadrupole Field Calculations

The three dimensional solution was done with the code TOSCA<sup>6</sup>. The effects of the shape of the end coil geometry and pole saturation were looked at since it is the integral multipole content that we must satisfy. As a starting point the magnet was modeled with no shaping of the poles at the end or use of field clamps to contain the field fall off. A well defined mesh was set up in the x,y plane using quadratic elements to obtain reasonable fits to the vector potential within the aperture of the magnet. This mesh was then extruded out along the z-axis with emphasis placed near the end of the magnet yoke and the region where the coils reside.

The post-processor OPERA<sup>7</sup> and the program EXTRACT<sup>8</sup> were used to analysis the integral multipole content of the magnet. The coefficients of a fourier fit to the total potential were integrated along the magnetic axis as a function of the radius. The analytic derivative of the potential was then taken to derive the coefficients for the magnetic fields. Figure 7 shows the field fall off along the magnetic axis for a radius of 30 cm. Table 4 list the results of the three dimensional study.

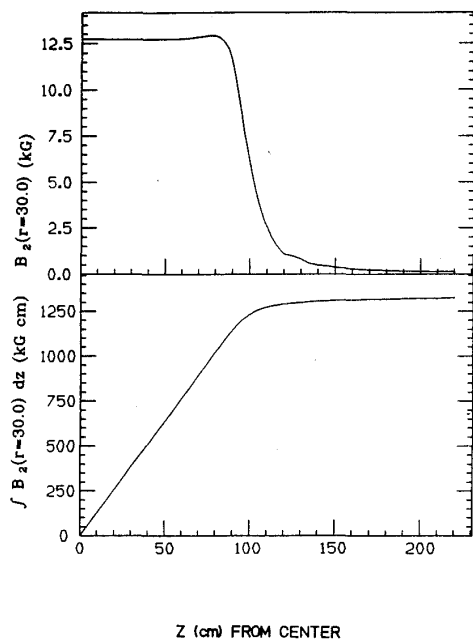


FIGURE 7. FIELD FALL OFF AND INTEGRAL OF QUADRUPOLE TERM

Table 4 Tosca Results and Parameters

Effective Length = 210 cm

B(N)	Integral [B(N) dz]	% of N=2
For R=35 cm (Pole Radius)		
B(2)	1.545 Tesla-m	
B(6)	5.62E-03 Tesla-m	0.364
B(10)	9.66E-03 Tesla-m	0.625
B(14)	1.05E-02 Tesla-m	0.682
For R=30 cm (Aperture Radius)		
B(2)	1.325 Tesla-m	
B(6)	2.77E-03 Tesla-m	0.209
B(10)	2.21E-03 Tesla-m	0.167
B(14)	9.23E-04 Tesla-m	0.070

The sum of the unknown multipoles (-ie- N=10 and 14) at the aperture of the magnetic is .237% of the quadrupole and the dodecapole is only .364% of the quadrupole at the pole. Studies will continue to investigate the effects of pole chamfering, field clamps and coil end geometries in regards to their contribution to the integral content.

#### Conclusion

A reference design has been modeled for the large aperture superconducting quadrupoles that meets the optical requirements of the High Momentum Spectrometer. It is our aim to complete the design work to allow a Request for Proposals to go out by December 1990.

#### References

1. Conceptual Design Report Basic Experimental Equipment - Hall C. April 13, 1990.
2. P.D. Brindza et al., "CEBAF Superconducting Spectrometer Design", *IEEE Transaction on Magnets*, Mag-25, 1897, 1989.
3. L.H. Harwood, et al., "A Superconducting Iron-Dominated Quadrupole for CEBAF", *IEEE Transaction on Magnets*, Mag-25, 1910, 1989.
4. POISSON MANUAL
5. J.A. Miller, et al., "Cryostat Design And Magnetostatic Analysis of the 6 Gev Superconducting Dipole for the High Momentum Spectrometer", *Submitted to IEEE Transaction on Magnets*.
6. TOSCA, *Vectra Fields Limited*
7. OPERA, *Vectra Fields Limited*
8. J. Napolitano et al., "Calculations of Higher Multipole Components in a Large Superconducting Quadrupole Magnet", *Submitted to Nuclear Instruments and Methods*.